International Journal of Fluid Power 3 (2002) No. 1 pp. 33-46

PRESSURE COMPONENTS STABILITY ANALYSIS: A REVISITED APPROACH

Marc Alirand[1], Gwennaël Favennec[1] and Michel Lebrun[2]

[1]Imagine SA, 5 rue Brison, 42300 Roanne, France, [2]Université Claude Bernard, 69000 Villeurbanne, France
alirand@amesim.com, favennec@amesim.com, lebrun@amesim.com

Abstract

In this paper the stability of pressure relief valves and pressure reducers is analysed. MacCloy and Merritt have previously proven that the stability analysis of these two components can be viewed with the same calculation. The purpose of this paper is to extend their results to other pressure control components and to add some other views of stability analysis using a simplification of the dynamics linked to the generally small volume of the counter reaction chamber. This simplification leads to a third order transfer function, which is easier to analyse. The static behaviour of both the pressure relief valve and the pressure-reducing valve is explained using this transfer function. A proof is given that the eigenvalues are heavily coupled using the roots calculation of a third order polynomial function. The analysis shows that the inner mechanical control loop of these two components can be viewed as a PD force controller. Root loci are used to understand the stability influences of certain design parameters. Other basic rules are also established.

Keywords: pressure relief valve, pressure reducing valve, stability problems, force control, pressure components

This manuscript was received on 9 October 2001 and was accepted after revision for publication on 3 April 2002

1 Introduction

Pressure control components such as relief and reducing valves play an essential role in many hydraulic circuits. In spite of their simple structure, such components are rather unstable and often excite vibrations that will be the cause of noise, disturbance of the normal operation and damage. Even today the development and optimisation of pressure components is a complex problem that requires a relatively large amount of experimental testing. Some of the reasons for this are the various flow conditions that the variable and fixed orifices experience, the wide range of applications regarding the controlled volumes and pressure levels, the design that results sometimes in small moving spool with classically low damping effect, the non-linearities of the system and more. Analytical analysis when it is possible to carry out, is important since it can help understand the influence of certain parameters directly on the dynamic behaviour and therefore reduce the development risks by a direct sizing validated using non-linear simulations. Even if linear models are based on sometimes crude assumptions, they are relevant in most applications of a first level of the dynamic behaviour. In this paper such an analysis is carried out and has shown promising results. Another interesting result is that either the pressure control component is a pressure reducing valve, a pressure relief valve, a check valve or a pressure servovalve, the stability analysis can be done in the same way using a third order transfer function.

Pressure reducers and pressure limiters are all pressure components. Generally speaking, they control with the help of spool equilibrium, the outlet pressure versus a pilot part which can be actuated mechanically (a spring preload), electrically (a direct action) or pilot operated from a smaller hydraulic valve. Merritt (1967) has presented the technologies of pressure components schematically by two sketches containing the same internal parts as presented in figures 1 and 2.

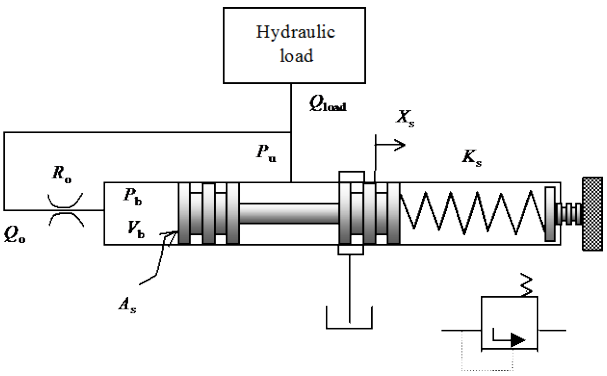

Fig. 1: *Pressure relief valve*

There exist fundamental differences between pressure limiters and pressure reducers. The pressure limiter is a component in parallel with the main circuit and it is normally closed. Conversely, the pressure reducer is in series with the main circuit and is normally open. A flow rate always exists in these components.

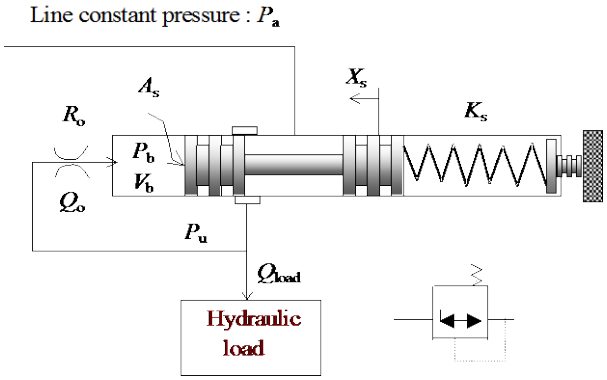

Fig. 2: *Pressure reducing valve*

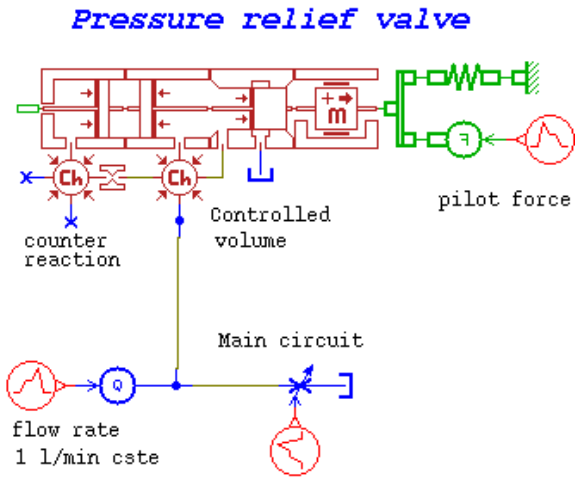

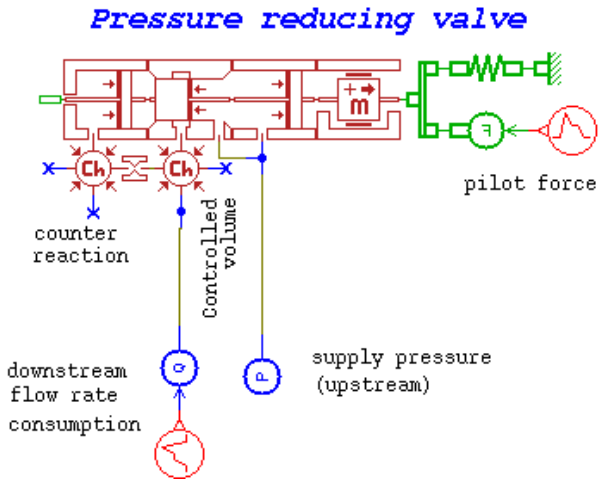

Fig. 3: *Pressure relief valve and reducing valve in AMESim*

As can be seen on Fig. 1 and 2, the systems are mainly the same. Only the controlled pressure changes. Pressure control valves employ feedback and may be properly regarded as a servo control loop: the controlled pressure is sensed on the spool valve and compared to a spring preload (in Fig. 1 and 2).

A non-linear model was developed first to compare the dynamics of these two systems. The models within AMESim are shown Fig. 3.

The two systems: the pressure relief valve and the reducing valve have the same parameters values. The regulation has been defined to be equal for the pressure equilibrium point to:

$$P_{util} = \frac{F_{cmd}}{A_S} = \frac{80\ \text{N}}{\frac{\pi}{4} 1^2\ \text{cm}^2} = 10.18\ \text{bar} \qquad (1)$$

The controlled pressure P_u for the pressure limiter is shown Fig. 4 and the controlled pressure in the reducing valve is shown Fig. 5.

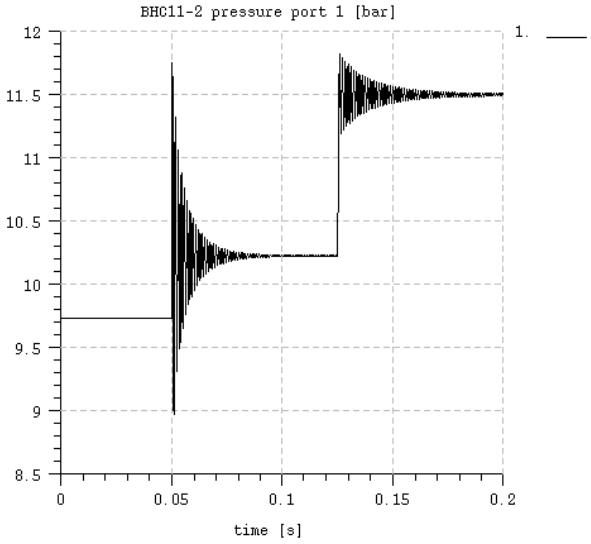

Fig. 4: *Relief valve controlled volume pressure*

For the relief valve, the input is a sudden closure of the main circuit restriction at time 0.05 s leading to a crossing flow rate of 1 l/min and a piloted force input of 10 N at time 0.125 s.

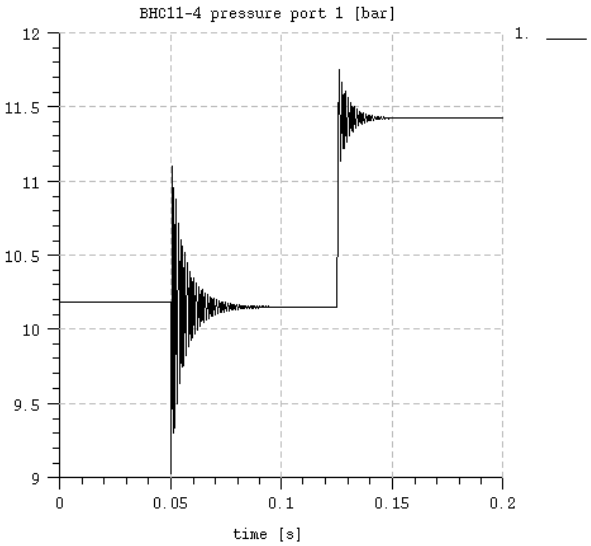

Fig. 5: *Reducing valve controlled volume pressure*

Table 1: Eigenvalues for both pressure components

Real part	Imaginary part	Damping ratio	Frequency
-133.09608	-4804.71347	0.02769	764.98724
-11.09608	4804.71347	0.02769	764.98724
-117.05583	4833.16874	0.02421	769.44827
-117.05583	-4833.16874	0.02421	769.44827
-12329.30425		1.00000	1962.26972
-12368.82825		1.00000	1968.56016
-420957.98590		1.00000	66997.54429
-429491.85850		1.00000	68355.75230

For the pressure reducer, the input is a sudden flow rate consumption of 1 l/min in the downstream circuit at time 0.05 s and a piloted force input of 10 N at time 0.125 s.

From the dynamics point of view, the responses for perturbations look the same as expected from Merritt (1967) and MacCloy (1980) results. The dynamics for both the systems are the same around the same operating points, here at time 0.1 sec corresponding to a crossing flow rate of 1 l/min for both components. The eigenvalues of both systems are very similar (see Table 1).

This linear analysis was done numerically, now starting from the non-linear model, the equations of the linear models of both the pressure components will be obtained and their block diagrams deduced. A simplification is carried out to obtain a third order characteristic equation of the states able to be analysed in "simple" ways. Some standard linear analyses are carried out on the simple linear model to have a look on the stability of these pressure control components. However the stability is not the only objective. It will be proven that the simplified linear model can also be applied to check valves and pressure servo valves.

2 Equations of Motion and Linearisation

To understand the dynamic behaviour and the stability of a pressure limiter or a pressure reducer, a linear analysis of these two components should be done. To do so the equations of motion for first the pressure limiter will be established starting from the bond graph of the pressure limiter shown in Fig. 1.

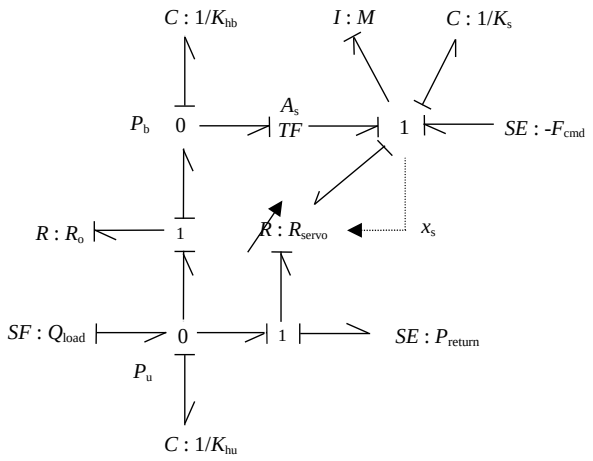

Fig. 6: *Pressure relief valve bond graph*

This technique is now well introduced and has been used by Lebrun (1987), Margolis (1997), Matsubara (2001) and Suzuki (1999) to represent standard hydraulic components. This technique is very useful when a component uses different Physics domains like electrical, magnetic, hydraulic and mechanical domain such as piloted pressure control components. Starting from this bond graph, the non-linear motion equations are obtained.

$$M\,\ddot{x}_s = -(F_{cmd} + K_{spring}\,x_s) - F_{jet} + A_{spool}\,P_{back} \tag{2a}$$

$$Q_s = C_q A(x_s)\sqrt{\frac{2}{\rho}P_{util}} \tag{2b}$$

$$Q_{orif} = C_q A_{orif}\sqrt{\frac{2}{\rho}(P_{util} - P_{back})} \tag{2c}$$

$$P_{back} = K_{hback}\int (Q_{orif} - A_{spool}\,\dot{x}_s)dt \tag{2d}$$

$$P_{util} = K_{hutil}\int (-Q_{orif} - Q_s + Q_{load})dt \tag{2e}$$

The Bernoulli non-linear equation of the flow rate crossing the component when it is opened should be linearised using independent variables. Generally speaking these independent variables are the state variables. Considering x_s and ΔP as the only two independent variables, the previous equation of Q_s can be rewritten as:

$$Q_s^* = C_q \pi D_s\sqrt{\frac{2}{\rho}\Delta P^0}\,x_s^* + C_q \pi D_s x_s^0 \frac{1}{\sqrt{2\rho\,\Delta P^0}}\Delta P^* \tag{3}$$

with the assumption that the flow is only turbulent and thus the discharge coefficient C_q is constant. ${x_s}^0$ and ΔP^0 are the equilibrium points for the linearisation. In order to simplify the presentation, the pressure relief valve is considered to be built with an annular cross section. For simplicity the previous linearised equation can be expressed more straightforward as:

$$Q_s^* = G_x x_s^* + G_{\Delta P}\Delta P^* \tag{4}$$

G_x and $G_{\Delta P}$ are respectively called the flow gain

and the flow-pressure gain. In this case, ΔP only equals to the utilisation pressure P_u.

When the valve is opened a certain amount of flow crosses the valve. This flow rate generates a force called jet or flow force which tends to always close the spool valve. The non-linear equation giving the flow force is:

$$F_{jet} = \frac{\rho Q_s^2 \cos\alpha}{C_q A(x_s)} \tag{5}$$

with cosα the cosine of the jet angle coming from the angle of the flow direction axis and the spool axis. Note that in this equation only the quasi-static flow force is kept. MacCloy (1980) used the transient flow forces in his spool equilibrium. From MacCloy (1980) and Baudry (2000), the contribution of the transient flow forces can have adverse contribution depending if the jet enters or exits from the valve. However, from Mare (1993), its contribution is generally negligible. Using the Bernoulli's non-linear equation of the flow rate, the linearised expression of the quasi-static flow force can be given by:

$$F_{jet}^* = 2\, C_q\, \pi\, D_s\, \cos\alpha\ \Delta P^0 x_s^* + 2 C_q\, \pi D_s\, \cos\alpha\ x_s^0\, \Delta P^* \tag{6}$$

which can be rewritten more straightforward in:

$$F_{jet}^* = K_{jet} x_s^* + A_{jet} \Delta P^* \tag{7}$$

The term function of x_s* corresponds to a relation between a force and a displacement. This term can be considered as stiffness and thus plays the same role as the spring. The term function of ΔP* corresponds to a relation between a force and a pressure. Thus this term can be considered as an equivalent area.

The remaining problem is to know the flow characteristic in the fixed orifice (the counter reaction restriction). The flow characteristic is mainly laminar due to the very low-pressure drop, and consequently the small velocity in the restriction. The discharge coefficient C_q is a function of the flow number λ as given by MacCloy (1980). This curve is coded in AMESim with:

$$C_q = C_{qmax} \tanh\left(\frac{2\lambda}{\lambda_{crit}}\right) \tag{8}$$

The laminar part corresponds to a linear function between the discharge coefficient C_q and the flow number λ:

$$C_q^* = C_{qmax} \frac{\partial}{\partial\lambda} \tanh\left(\frac{2\lambda}{\lambda_{crit}}\right)\bigg|_{\lambda=0} \tag{9a}$$

$$\lambda^* = \frac{2C_{qmax}}{\lambda_{crit}} \lambda^* \tag{9b}$$

With the flow number definition, the Bernoulli equation in the fixed restriction becomes:

$$Q_{orif} = \frac{2C_{qmax}}{\lambda_{crit}} \frac{d_h}{\nu} A_r \frac{2}{\rho}(P_u - P_b) = \frac{P_u - P_b}{R_{orif}} \tag{10}$$

Combining all equations and expressing them in a block diagram lead to Fig. 7.

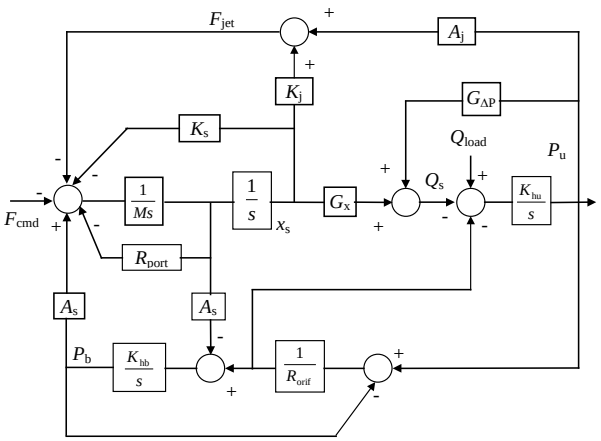

Fig. 7: *Pressure relief valve block diagram*

This block diagram represents almost the same block diagram obtained by Merritt (1967), MacCloy (1980) and Manring (1997) except that it is not as compact. In order to compare the dynamics of a pressure relief valve and the ones of a pressure-reducing valve, the motion equation of the pressure-reducing valve should be calculated. Once again a bond graph is used (Fig. 8).

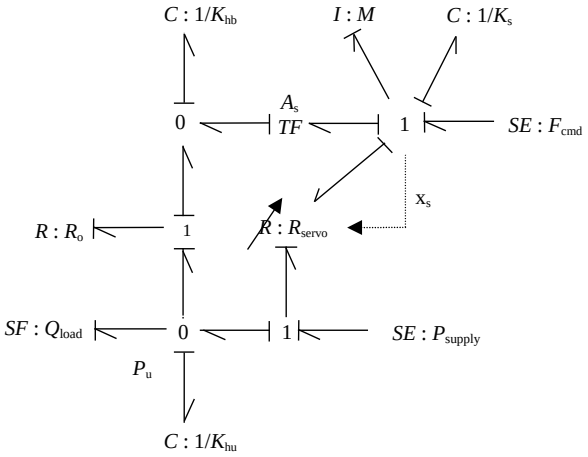

Fig. 8: *Bond graph of the pressure reducing valve*

From this bond graph, the non-linear dynamic equations of the pressure reducer are obtained as:

$$M\,\ddot{x}_s = F_{cmd} - K_{spring}\, x_s - F_{jet} - A_{spool}\, P_{back} \tag{11a}$$

$$Q_{servo} = C_q A(x_s) \sqrt{\frac{2}{\rho}(P_{supply} - P_{util})} \tag{11b}$$

$$Q_{orif} = C_q A_{orif} \sqrt{\frac{2}{\rho}(P_{util} - P_{back})} \tag{11c}$$

$$P_{back} = K_{hback} \int (Q_{orif} + A_{spool} \dot{x}_s) dt \tag{11d}$$

$$P_{util} = K_{hutil} \int (-Q_{orif} + Q_{servo} - Q_{load}) dt \tag{11e}$$

Using the same techniques as before the governing linear equations are combined into the block diagram

Fig. 9.

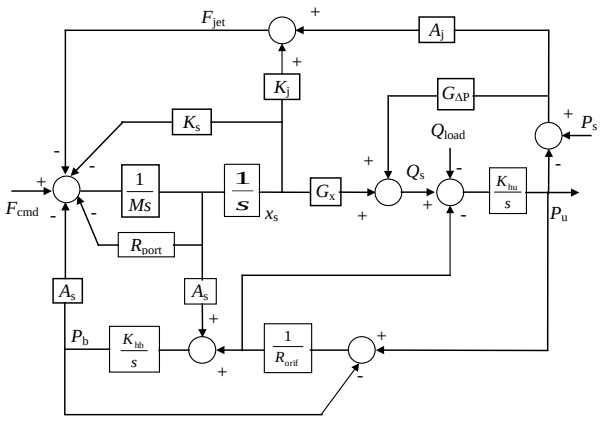

Fig. 9: *Pressure reducer block diagram*

The differences between the two components are coming from the flow rate crossing the variable restriction and the pressure counter reaction. This is also shown on the two bond graphs Fig. 6 and 8. They are exactly the same except for the power directions of some bonds: the pressure counter reaction and the flow rate in the valve. From a bond graph point of view, this means that the dynamics of the linear model obtained from these two bond graphs are the same. From a transfer function point of view, this means that the denominators are the same but the numerators can be different.

3 Simplification

The analysis of the eigenvalues in Table 1 shows a high dynamic. This high dynamic is linked to the volume of the counter reaction chamber. MacCloy (1980) and Merritt (1967) have kept this high dynamic for their analysis. However and as mentioned by Merritt (1967), the hydraulic stiffness of the counter reaction chamber is generally very high regarding the hydraulic stiffness of the controlled volume and the equivalent hydraulic stiffness of the spring. Thus it is possible to simplify this dynamic. This has been done by Alirand (2001) using a bond graph technique and also Handroos (1990) and Maiti (1999). For simplicity, this comes from the fact that, below a limit frequency, the counter reaction pressure does not vary except when P_u varies and the flow rate crossing the fixed restriction is exactly the flow rate induced by the spool motion. That is to say:

$$Q_{orif} = A_s \dot{x}_s \tag{12}$$

Now using the equation of the relief valve and modifying the causality of the flow rate equation (Eq. 10) in the counter reaction restriction into

$$P_b = P_u - R_o Q_o = P_u - R_o A_s \dot{x}_s \tag{13}$$

and replacing the counter reaction pressure P_b into the spool equilibrium equation leads to:

$$M\,\ddot{x}_s = -(F_{cmd} + K_s x_s) - F_j + A_s (P_u - A_s R_o \dot{x}_s) \tag{14}$$

This modification in the state equations eliminates the pressure P_b. The pressure senses on the spool end area is now the controlled pressure P_u. Thus the pressure P_u counter reacts on the spool via the spool area but also counter reacts by the equivalent area of the jet force effect. These two contributions are in the opposite direction for the two pressure valves. It should be noted here that the contribution of the equivalent jet force section could be neglected versus the spool section. The comparison has to be done between $\pi \cdot D_s^2/4$ and $2 \cdot C_q \cdot \pi \cdot D_s \cdot \cos\alpha \cdot x_s$. This equivalent section can be removed from the two previous block diagrams. The term R_{port} corresponding to a viscous friction has been also removed because it is very small regarding the orifice damping effect (usually).

The explanations given here come from a more general bond graph automatic simplification technique based on stored and dissipated energy in elements in-

troduced by Rosenberg (1988) and Louca (1997). The simplified bond graph of the pressure relief valve is shown in Fig. 10 since it will be used later on for the check valve.

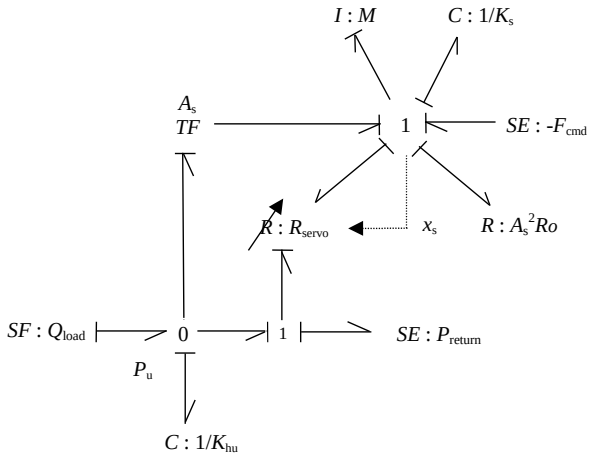

Fig. 10: *Pressure relief valve simplified bond graph*

Adding the two spring effects and reorganizing the pressure relief valve block diagram leads to Fig. 11.

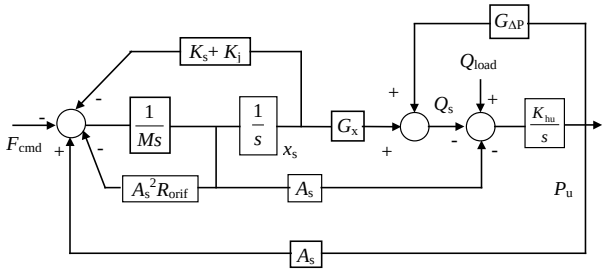

Fig. 11: *Pressure relief valve simplified block diagram*

This block diagram can be reorganized once more in a simpler way to build transfer functions and has a look on the control loop. The final block diagram is the one shown in Fig. 12.

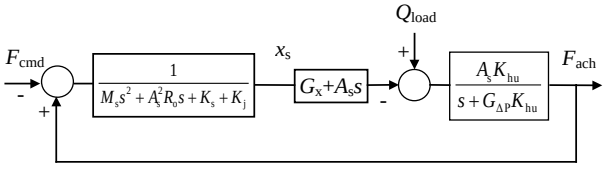

Fig. 12: *Pressure relief valve simplified block diagram*

Using the same technique for the pressure reducer leads to the block diagram Fig. 13.

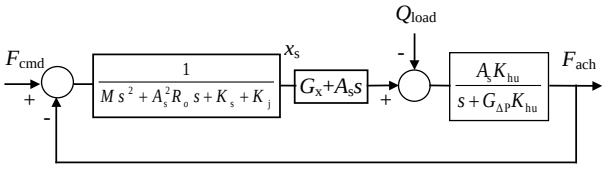

Fig. 13: *Pressure reducing valve simplified block diagram*

In order to validate the simplification, a linear model has been built within AMESim (Fig. 14) and compared to the simulation results of the previous non-linear model of the pressure relief valve.

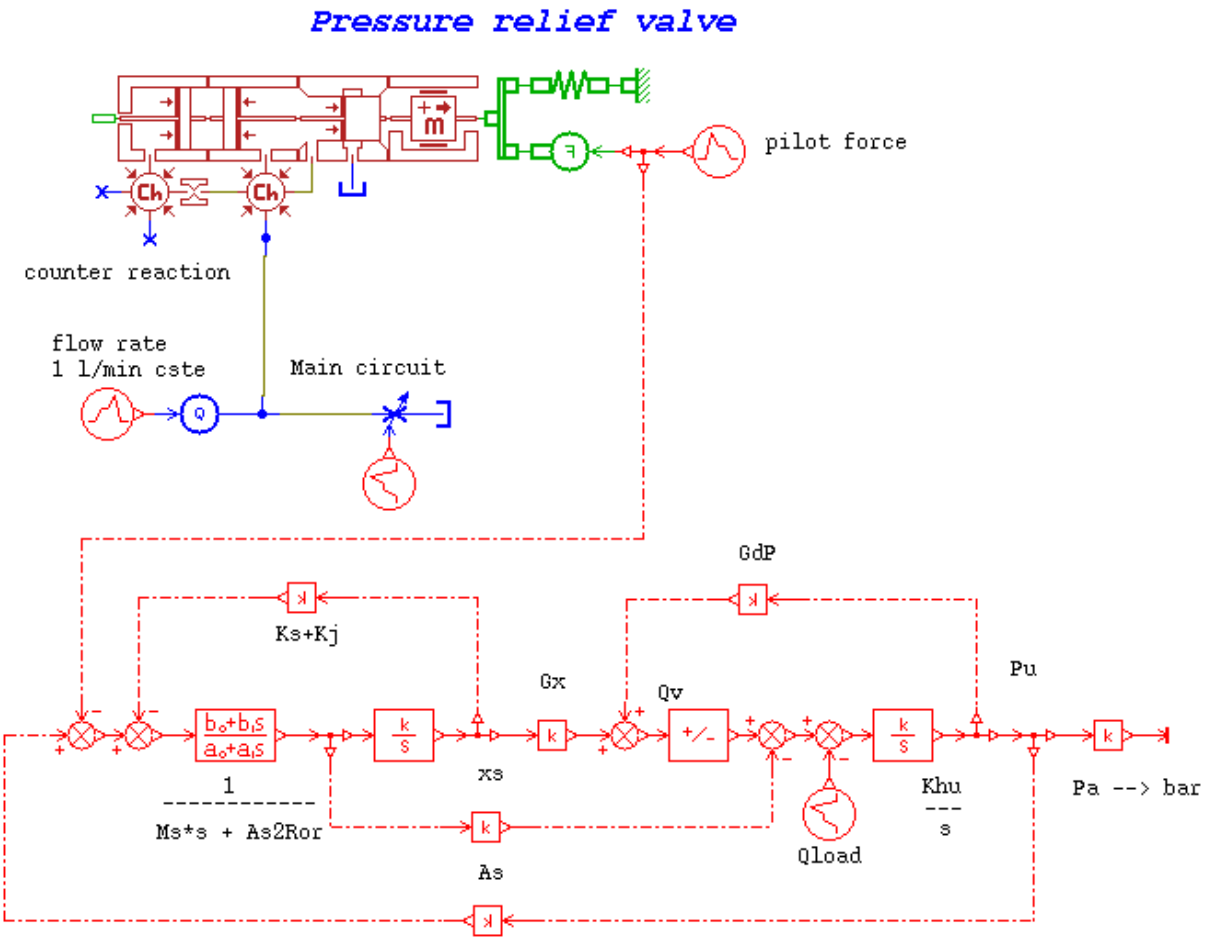

Fig. 14: *Relief valve – non-linear and linear model*

The eigenvalues for both the models are given in Table 2.

As expected, they are almost the same and the high frequency mode has been removed from the linear model. The time response of the linear model and the non-linear model are thus expected to be the same (see Fig. 15). The input is a pure step of force of 10 N and not a filtered step input in order to show some oscillations.

Table 2: *Eigenvalues - non linear and linear model*

Real part	Imaginary part	Damping ratio	Frequency
-116.26043	-4834.56778	0.02404	769.66781
-116.26043	4834.56778	0.02404	769.66781
-140.91091	-4887.54039	0.02882	778.19943
-140.91091	4887.54039	0.02882	778.19943
-12056.87028		1.00000	1918.91050
-12364.85228		1.00000	1967.92736
-421136.16820		1.00000	67025.90288

These results validate the simplification: the elimination of the high frequency mode does not affect the low modes and the time response. The differences between the oscillations (Fig. 15) are due to the fact that since the controlled pressure increases, the spool is less opened. The equilibrium point is modified and thus the modes. This validation has been carried out on the relief valve but can be done on the pressure reducer.

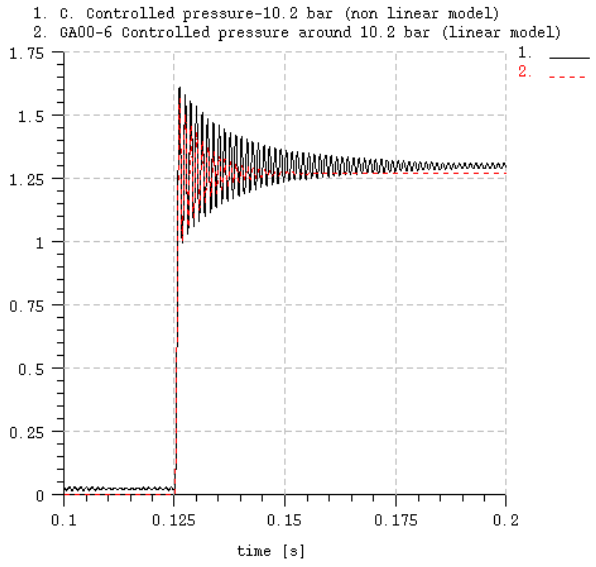

Fig. 15: *Comparison linear and non-linear model*

4 Analysis

From the block diagrams Fig. 12 and 13, the same transfer function of the controlled pressure is obtained:

$$P_u = \frac{K_{hu}(A_s s + G_x)F_{cmd} \pm K_{hu}(M s^2 + A_s^2 R_o s + K_s + K_j)Q_{load}}{(s + G_{\Delta P} K_{hu})(M s^2 + A_s^2 R_o s + K_s + K_j) + A_s K_{hu}(A_s s + G_x)} \quad (15)$$

From this transfer function it is clear now that both systems are identical from the dynamics point of view. Only the numerators are different and this, depending on the system: a pressure relief valve ($+Q_{load}$) or a pressurereducing valve ($-Q_{load}$).

It is also clear from Fig. 12 and 13 that these two systems contain a mechanical inner loop (i.e. a feedback) and thus should be regarded as mentioned by Merritt (1967) as servo control systems.

An interesting aspect of a control loop is its static error. For both components, the previous transfer function gives:

$$\left.\frac{P_u}{F_{cmd}}\right|_{s=0} = \frac{1}{A_s + \dfrac{G_{\Delta P}(K_s + K_j)}{G_x}} \quad (16)$$

This clearly shows a static error due to the "fictitious" leakage $G_{\Delta P}$, the spring stiffness and the flow forces effect. This static error can also be viewed from the valve flow rate input or output depending on the type of valve. It corresponds to the standard characteristic curves normally given by any valve manufacturers.

From a control point of view, the load flow rate is a perturbation. The system should at least be independent in steady state regarding this perturbation. However a classical characteristic of a pressure limiter is the one shown Fig. 16.

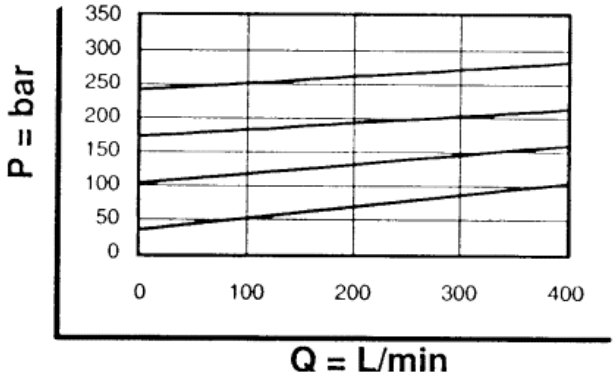

Fig. 16: *Relief valve characteristic curve (from SUN)*

This characteristic should be as flat as possible. When the system opens and whatever the flow rate through it is, the controlled pressure should be the same and be given by the pilot. Such a resulting curve can be explained by the spring and flow force effects. The characteristic Fig. 16 can be viewed as the transfer function between the input flow rate Q_{load} and the controlled pressure P_u. The previous transfer function leads to

$$\left.\frac{P_{util}}{Q_{load}}\right|_{s=0} = \frac{1}{\dfrac{A_s G_x}{K_s + K_j} + G_{\Delta P}} \quad (17)$$

Without spring and flow forces, the static value of the previous transfer function will be zero. The more the flow rate crosses the valve, the more the controlled pressure is. When the input flow rate increases, this flow rate should be eliminated via an increase of the valve opening. It compresses the spring and thus leads to an increase of the pilot force. This explains the spring effect. For the flow force effect, since the flow rate increases the flow forces also increase. Consequently the spool tends to close and the equivalent pilot force viewed from the spool also increases. This explained firstly the characteristic curve of a pressure relief valve and secondly the linear static error. One should note that the section A_{jet} has been removed from the equations. Its contribution reduces the force due to the counter reaction. The pressure counter reaction needs to be higher to equilibrate the valve spool and thus this linear phenomenon also leads to a static error.

For a pressure reducer, standard characteristic curves have been shown in Fig. 17.

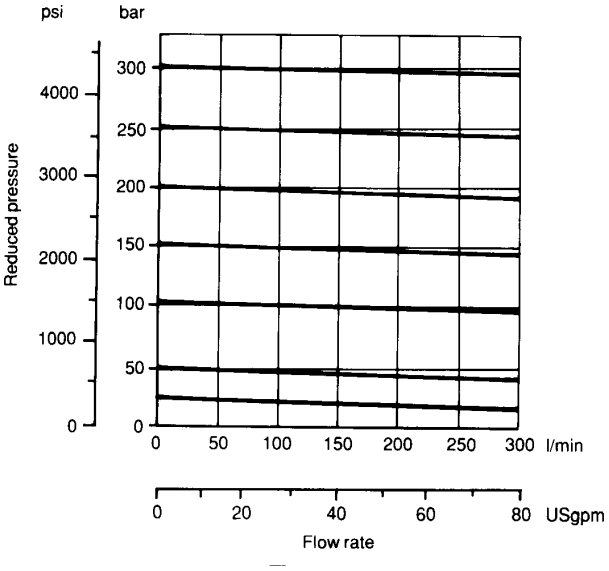

Fig. 17: *Pressure reducer characteristic curve (from VICKERS)*

For the pressure reducer the same technique is used and thus the static value of the transfer function between the controlled pressure and the load flow rate Q_{load} is given by:

$$\left.\frac{P_{util}}{Q_{load}}\right|_{s=0} = \frac{-1}{\dfrac{A_s G_x}{K_s + K_j} + G_{\Delta P}} \quad (18)$$

The negative sign explains the fact that increasing the crossing flow rate decreases the controlled pressure. The same explanations are given: increasing the load flow rate increases the flow forces but these forces make the equivalent pilot force decreasing (opposite effects for the relief valve). Conversely, increasing the

load flow rate opens the cross section and thus the spring force decreases. The controlled pressure decreases in both conditions since the equivalent pilot force decreases. This explains the characteristic of a pressure reducer.

The most important aspect of a control loop is its stability and consequently the calculation of the eigenvalues. One should note that since the denominator of the transfer function is a third order, it should be possible to express analytically its solutions and thus know the exact values of the RC mode and the oscillating mode. Unfortunately this is only theoretical. Firstly, it is difficult from the previous equation to calculate by hand the zeros of the transfer function denominator. Secondly, when this is done, the terms are generally too coupled together which makes it difficult to conclude on the action of a particular term on the frequencies and damping involved.

In order to have an idea of this complexity, the denominator is modified into a normalized form to be easily solved:

$$D(s) = s^3 + \frac{M\,G_{\Delta P}\,K_{hu} + A_s^2\,R_o}{M}\,s^2 + \frac{K_s + K_j + A_s^2\,K_{hu} + A_s^2\,R_o\,G_{\Delta P}\,K_{hu}}{M}\,s + \frac{K_{hu}\left(G_{\Delta P}\left(K_s + K_j\right) + A_s\,G_x\right)}{M} \tag{19}$$

This should be compared to the equation:

$$D(s) = s^3 + a_2 s^2 + a_1 s + a_0 \tag{20}$$

Using the classical technique to factorise a third order equation:

$$Q = \frac{3a_1 - a_2^2}{9} \tag{21}$$

$$R = \frac{9a_2a_1 - 27a_0 - 2a_2^3}{54} \tag{22}$$

by substitution leads to

$$Q = \frac{K_s + K_j + A_s^2\,K_{hu} + A_s^2\,R_o\,G_{\Delta P}\,K_{hu}}{3M} - \left(\frac{M\,G_{\Delta P}\,K_{hu} + A_s^2\,R_o}{3M}\right)^2 \tag{23}$$

$$R = \frac{\left(M\,G_{\Delta P}\,K_{hu} + A_s^2\,R_o\right)\left(K_s + K_j + A_s^2\,K_{hu} + A_s^2\,R_o\,G_{\Delta P}\,K_{hu}\right)}{6M^2} - \frac{K_{hu}\left(G_{\Delta P}\left(K_s + K_j\right) + A_s\,G_x\right)}{2M} - \frac{\left(M\,G_{\Delta P}\,K_{hu} + A_s^2\,R_o\right)^3}{27M^3} \tag{24}$$

These two values are difficult to simplified: there is no simple equation manipulations to eliminate terms and generally no approximation can be done, as the contributions of each elements are very similar. However note that some exceptions exist for particular cases. Using the discriminant defined as:

$$\Delta = Q^3 + R^2 \tag{25}$$

it is difficult to obtain a clear idea of the eigenvalues and what are the main parameters that participate in each eigenvalues.

It is also possible to use the fact that the solutions are a real part and two complex conjugated parts. If $s_1 = -z'\omega$ is the real part and s_2 and s_3 defined by:

$$s_2, s_3 = -z\omega \pm j\sqrt{1 - z^2}\,\omega \tag{26}$$

are the two complex parts, a new system of equations is obtained

$$s_1 + s_2 + s_3 = -\omega(z' + 2z) = -a_2 \tag{27a}$$

$$s_1(s_2 + s_3) + s_2 s_3 = \omega^2(2zz' + 1) = a_1 \tag{27b}$$

$$s_1 s_2 s_3 = -z'\omega^3 = -a_0 \tag{27c}$$

If the first equation is used to expressed the sum of the complex poles and replaces it in the second equation this leads to:

$$-s_1(s_1 + a_2) + \omega^2 = a_1 \tag{28}$$

and using the third equation to express s_1 function of ω yield:

$$\frac{a_0}{\omega^2}\left(-\frac{a_0}{\omega^2} + a_2\right) + \omega^2 = a_1 \tag{29}$$

which can be re-expressed as

$$\omega^6 - a_1\omega^4 + a_2 a_0 \omega^2 - a_0^2 = 0 \tag{30}$$

From this equation the natural frequency of the oscillating parts can be calculated but once more the calculation is very complex and cannot allow one to fully understand the influence of each parameters.

From these calculations the only clear thing is that the parameters are all coupled in all the eigenvalues. In order to analyse the stability of the two pressure components only classical means can be used.

One of the possibilities is to use the open loop gain and the parameters involved in. The gain of the inner loop of the previous block diagrams is given by

$$Gain = \frac{A_s\,G_x\,K_{hu}}{K_s + K_j} \tag{31}$$

This gain, in a certain sense, looks like the open loop gain. In any applications the two valves should work well and be stable independently of the controlled volume (i.e. the system upstream or downstream). This leads to possible stability problems if this gain is too high. Consequently reducing the flow gain G_x and increasing the flow forces and the spring stiffness contribute to stabilize the circuit. The spring stiffness and the flow forces have adverse effects because they improve the stability but they increase the static error. Also note that when these types of component have a flow force compensation, they start to be more difficult to design due to the stabilizing effect of the flow forces.

MacCloy (1980) and Margolis (1997) have analysed the stability problems using the Routh-Hurwitz criterion. This criterion gives a limit value that leads to stable system but oscillating. Manring (1997) has proposed to fix a desired time response. This time response allows specifying a lower limit value for the flow gain. However this technique does not guaranty a non-oscillating valve. Optimum values of such systems can

be achieved using a pole placement technique as described by Favennec (2001, 2002).

Another possibility to analyse the stability of a control loop is the roots location for parameter variations. Unfortunately a parameter variation on the non-linear model could not maintain the same operating point for all the variations due to non-linearities (G_x and $G_{\Delta P}$ are function of the operating point). Since the operating point has a great influence on the eigenvalues, it is impossible to use the non-linear model to make any analysis on the eigenvalues. Linear models are thus used even if they are not propagating solutions. They are able to give some aspects of the system stability around an operating point.

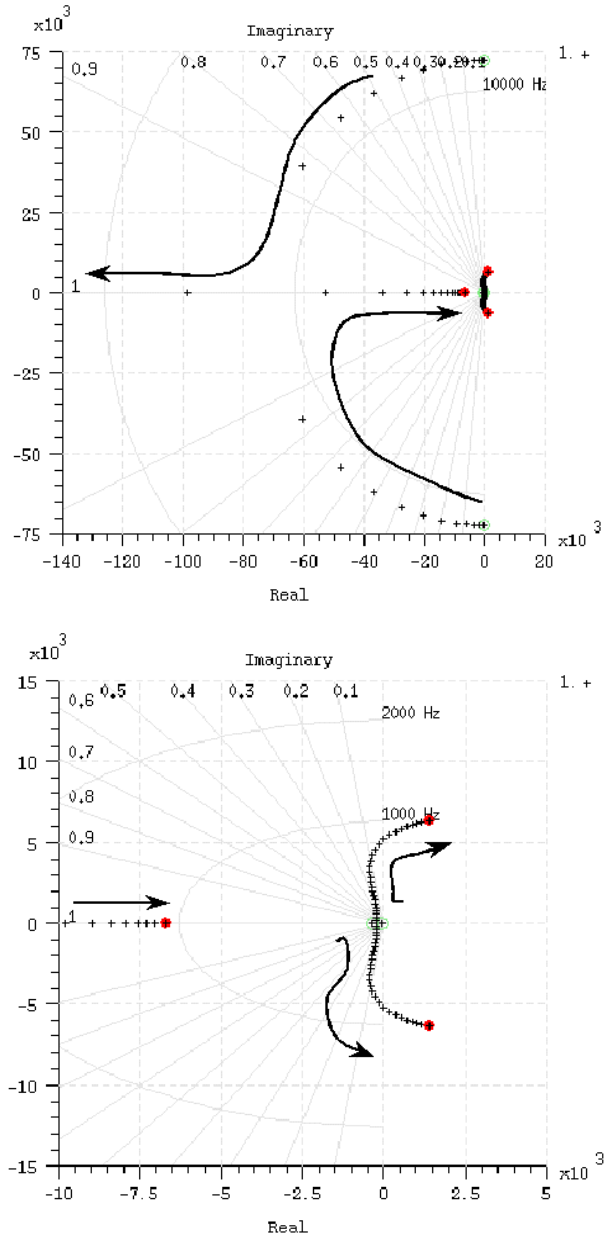

Fig. 18: *Root locus for a restriction diameter variation*

Merritt (1967) has shown that the counter reaction restriction has a stabilizing effect. However as shown by Alirand (2001), the restriction diameter has adverse contribution. When it is fully opened the system is not really stable and when it is closed there is no pressure control or the dynamics of the pressure control becomes very low. Figure 18 introduces the evolution of the roots for variation of the counter reaction restriction diameter from 0.1 mm to 1.5 mm (respectively beginning of the arrow and end of the arrow in Fig. 18). Note that the variation uses the block diagram Fig. 7 and thus the complete linear model.

The limits of these root loci are defined by two separate cases:

- $R_o \rightarrow \infty$ (very small orifice diameter)
  The denominator of the transfer function coming from the block diagram Fig. 7 is given by:
  $$D(s) = \left(M\, s^2 + K_s + K_j + A_s^2\, K_{hb}\right)\left(s + G_{\Delta P}\, K_{hu}\right) \quad (32)$$
  and a null pole. This situation corresponds to the beginning of the arrows in Fig. 18. The system has no more pressure control since the restriction disconnects the counter reaction from the load. In this case, the hydraulic stiffness of the counter reaction chamber acts as if it was connected to a fixed part. The system thus has a very high frequency oscillating part.
- $R_o \rightarrow 0$ (fully opened orifice, i.e. big orifice diameter)
  In this case the load chamber is directly connected to the counter reaction chamber and an equivalent stiffness is due to the two previous ones in series (still noted K_{hu}). The denominator is now given by:
  $$D(s) = (s + G_{\Delta P} K_{hu})(Ms^2 + K_S + K_j) + A_S K_{hu}(A_S s + G_x) \quad (33)$$
  The ending arrows in Fig. 18 show the roots of this denominator. In this case, the system is composed of a low frequency time constant and a low frequency oscillating part.

From this, the restriction R_o has two opposite effects: if the restriction diameter is big, the counter reaction pressure quickly acts and as a result the force control is efficient but the spool valve could be not well damped. If the restriction is closed, there is not sufficient dynamics on the force control loop and unfortunately the valve spool is also not well damped. As a conclusion, the counter reaction restriction diameter is the easier element that can be adapted to correctly design a pressure relief and/or reducing valve. There exists a compromise on this diameter to have a good dynamic for the pressure control and a stable response.

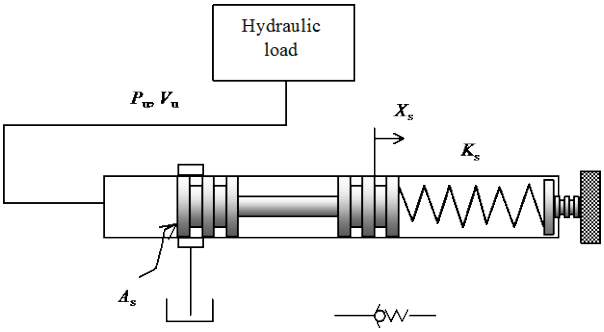

Fig. 19: *Check valve equivalent representation*

The structure of the denominator Eq. 33 exactly corresponds to the bond graph Fig. 10 with no dissipa-

tive element due to the fixed restriction R_o. This bond graph is also exactly the one of a check valve. The P_u pressure directly acts on the spool (or for poppet type valve on the ball or the conical element). If the pressure relief valve sketch in Fig. 1 is adapted to be compared to the one of a check valve using an annular cross section, such a modification can give the sketch shown in Fig. 19.

In this figure, the opening section location has been changed from the pressure relief valve sketch Fig. 1 and since the controlled pressure at the centre of the valve has no effect on the spool equilibrium (like for the pressure relief valve), the connecting line is removed to have the same aspect as a poppet valve. Note that the valve Fig. 19 has an annular cross section, which is not really standard for poppet valves.

Using this, the stability analysis of a check valve should be carried out using the transfer function denominator Eq. 33. Since check valves are simple pressure components very similar to pressure relief valves (except that they have no counter reaction restriction), they are particular cases of the more general transfer function of Eq. 15. As a consequence, the check valve using the same parameter values of the pressure relief valve Fig. 3 is normally unstable since it corresponds in Fig. 18 to some thing in the left half plane near the ending arrow (R_o equals 0, i.e., no fixed orifice or D_{orif} as bigger as possible).

Due to the comparison between a check valve and a relief valve, the counter reaction restriction is not the only way to stabilize a pressure control component.

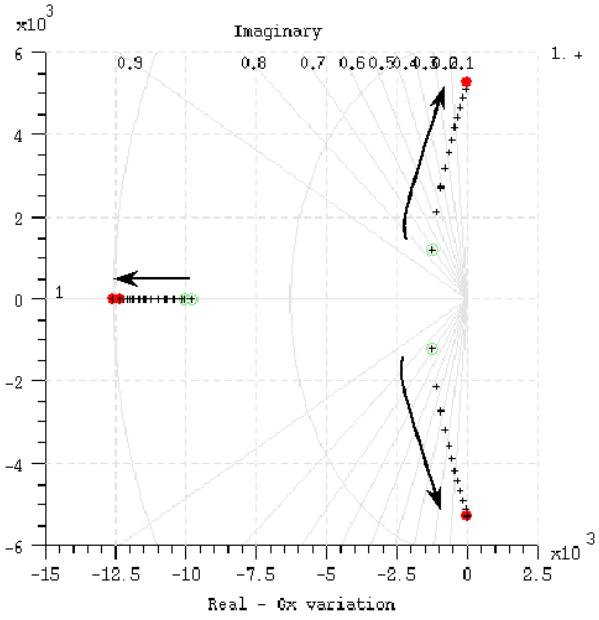

Fig. 20: *Root locus for a flow gain variation*

Manring (1997) has analysed the effect of the geometry of the opening section on the stability of a relief valve. He shows the great effect of the flow gain G_x. As presented before, the flow gain directly affect the inner loop gain and thus a low value of flow gain may stabilize a pressure component. Figure 20 corresponds to a variation of the flow gain from 0.1 to 1.2 times the existing flow gain (respectively beginning of the arrow and end of the arrow in Fig. 20). This figure also shows a stability improvement. Decreasing the flow gain tends to stabilize the valve and as expected slows down the system dynamic response.

In Fig. 20 the variation of the flow gain was done for the complete and simplified linear models. As can be seen, the roots of the fourth order denominator and the roots of the third order denominator agree. This also shows that when the assumptions for the simplification are valid, the two models (of fourth order and third order) produce the same root locus.

The flow-pressure gain $G_{\Delta P}$ can be viewed from the block diagrams as a leakage and thus has the same effects. Since it corresponds to a damping effect, increasing the leakage or the flow-pressure gain tends to stabilize the valve. From a stability analysis point of view, this term can be removed since if the system is stable without this term, the system should be more stable with it.

As previously said the flow forces are normally seen as a damper effect. The variation of the stiffness due to the jet force (Fig. 21) also shows a stabilization of the system even if the flow forces are no longer a damper effect in linear. In Fig. 21 the jet stiffness varies from the normal one to ten times the normal one.

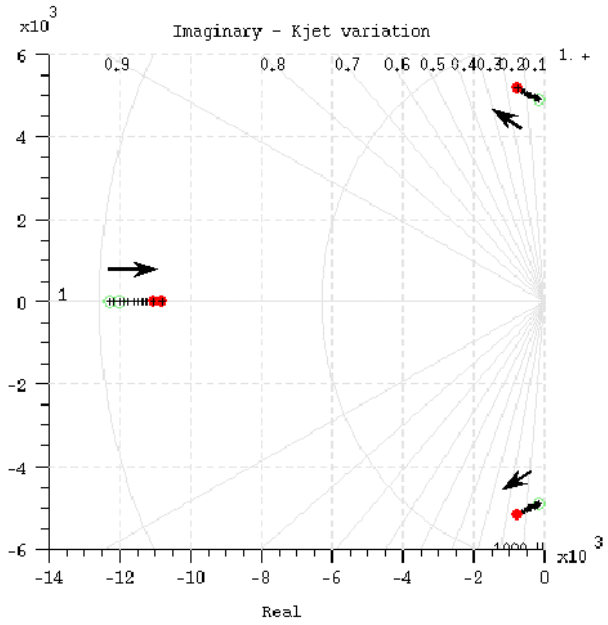

Fig. 21: *Root locus for flow force variation*

It should be noted that since the stiffness tends to stabilize the valve, increasing the spring stiffness has the same effect. However one should remember that increasing the flow forces and the spring stiffness increases the static error. Note that, once again, the simplified and the complete models are plotted on the same graph and give the same results.

Figure 22 comes from Matsubara (2001). It shows the stability problem of a pressure valve expressed in a plane: pressure supply as *x*-axis and spool displacement as *y*-axis.

The axis of this plane corresponds to the operating point (x_s^0,ΔP^0) previously defined. These values affect

the flow gain, the flow-pressure gain and also the jet force terms. Increasing the supply pressure increases the value ΔP^0 and consequently increases the flow gain and the jet stiffness K_{jet}. In a same way increasing the spool displacement increases the flow-pressure gain. Note that this is only valid for an annular cross section and should be adapted for other geometry. However the tendencies shown in Fig. 22 can be explained by the previous stability analysis done on the root locus. A pressure component is generally unstable for high supply pressure (due to bigger flow gain) and small openings (due to smaller flow-pressure gain). However, due to the non-linearities of the flow rate and the flow forces, it is difficult to conclude for very small openings.

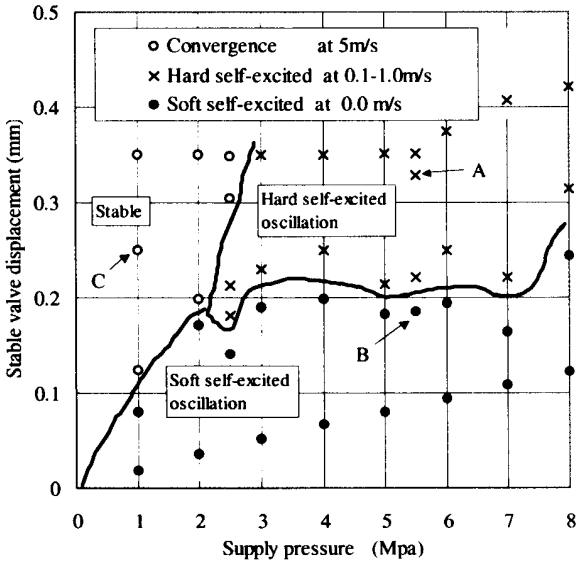

Fig. 22: *Stability region of a pressure valve (Matsubara, 2001)*

The last parameter variation is done on the volume of the hydraulic load V_{hutil}. For the variation shown in Fig. 23, the volume varies from 50 cm^3 to 500 cm^3.

As expected, if the controlled volume increases the frequency of the oscillating part decreases. Normally the oscillating part does not correspond to the hydro-mechanical mode of the spool given by:

$$\omega_{mec} = \sqrt{\frac{K_s + K_j + A_s^2 K_{hu}}{M}} \qquad (34)$$

since the system includes a control loop. However this calculation can give, in some cases like the one here, a good approximation. For this application, K_r = 1000 N/m, K_j = 17950 N/m and $A_s^2 K_{hu}$ = 209750 N/m with a controlled volume of 50 cm^3, this gives a natural frequency of 761 Hz which is close to the value obtained via the linear analysis. Note that the equivalent mechanical stiffness of the controlled volume is far higher than the others and thus approximations can be done.

Depending on the system to control, the valve can be slow or rapid and even may some times be unstable. A pressure component is consequently adapted to certain systems but cannot be applied to every hydraulic circuits. In this sense, even if pressure components are widely used in hydraulic circuits and are most of the time stable, depending on the downstream circuit, they can lead to chatter phenomena.

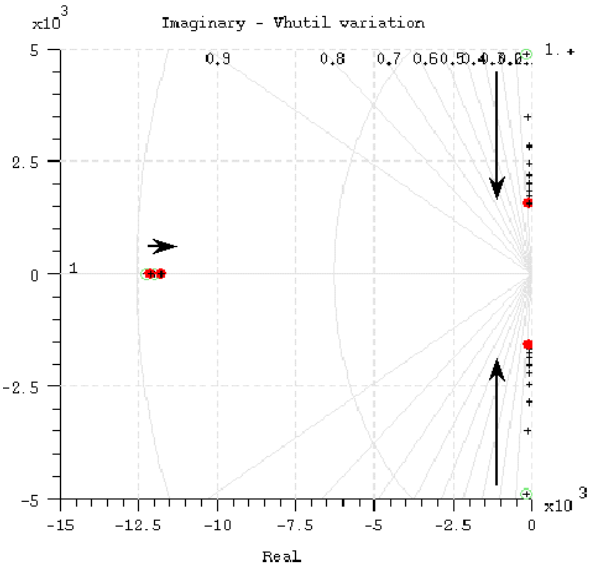

Fig. 23: *Root locus for controlled volume variations*

From another point of view, the previous block diagrams Fig. 12 and 13 can be rearranged once more into the one Fig. 24.

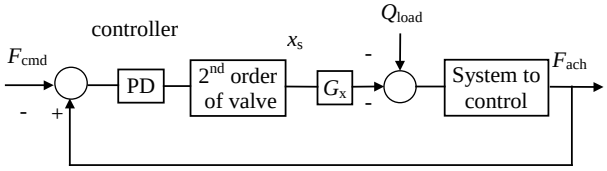

Fig. 24: *Equivalent block diagram for pressure valves*

From this figure the pressure component is similar to a force controller with proportional and derivative gains: the second order of the valve corresponds to the dynamics of a flow-controlled valve, the term G_x corresponds to the flow gain of a flow-controlled valve. Botelle (2000) has analysed such a control loop and a PI controller had been demonstrated to be better from the static error point of view. For a pressure control component, the “valve” dynamic comes from the spool and the counter reaction. Since this dynamic is far higher than the one of a flow-controlled valve can have, the delay due to the “valve” dynamic is less. Consequently and as shown by Alirand (2001), from a control point of view, it is better to use a pressure component to control a pressure or an effort than a flow controlled valve with an electronic control loop. One should note that the pressure “valve” dynamic is directly linked to the spool mass. Therefore and as mentioned by Green (1970) the spool mass should be as small as possible to increase the hydro-mechanical dynamic of the spool and thus have a very powerful counter reaction with no much delay.

As mentioned above, a pressure component always includes an inner PD control loop. The derivative effect can be used to stabilize the system. The open loop transfer function of the achieved force versus the input force is given by:

$$F_{ach} = \frac{A_s K_{hu}\left(A_s s + G_x\right)F_{cmd}}{\left(s + G_{\Delta P} K_{hu}\right)\left(M s^2 + A_s^2 R_o s + K_s + K_j\right)} \qquad (35)$$

If the zero of the numerator appears before the zero (the real part) of the denominator, the margin is more important and than the valve should be more stable. This is why generally speaking a spool with a bigger active section (the counter reaction section) leads to a system more stable if no change is done on the flow gain.

The last comment deals with pressure servo valves. A three-ways pressure servo valve may have the sketch shown Fig. 25.

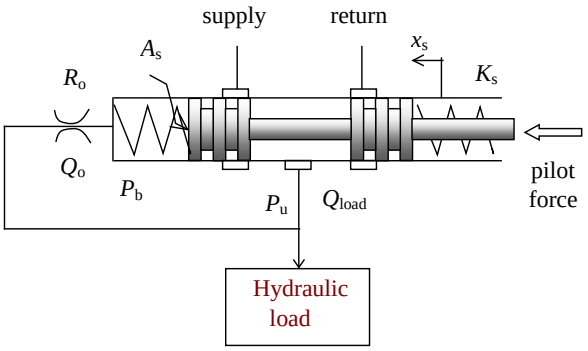

Fig. 25: *Pressure servovalve*

From this, the calculation of the transfer function of the controlled pressure versus the inputs also leads to a transfer function similar to Eq. 15. The stability of such components can also be deduced from the previous calculation since a pressure servo valve can be viewed as a combination of a relief valve and a reducing valve.

5 Conclusions

Starting from non-linear models, simplified linear models of pressure reducing and pressure relief valves were given. Their transfer function denominators are the same and are of third order type. The analysis of the denominator of the transfer functions has shown that it is difficult to obtain a clear idea of the contribution of each design parameters on the stability. Each roots of the denominator contain a heavily coupling of all the design parameters. Even if the simplification to a third order denominator seems to be of no much interest here, it will prove its interest in a companion paper done by Favennec (2002). One of the goals of this paper was to extend the conclusions of Merritt (1967) and MacCloy (1980) to other pressure control components.

The linear analysis has clearly shown that the stability of a pressure relief valve and a pressure-reducing valve are the same. It has also been shown that the stability of check valves and pressure servo valves can be done in the same way considering for the first one a value of R_{orif} equals to zero and for the other a coupling of both the reducing and relief valves.

Since pressure control components are clearly closed loop systems, stability analysis and static error are of importance. The static error is deduced from the transfer function of both components. The influences of the spring stiffness and the flow forces are clearly shown using the standard pressure/flow rate characteristic curves of pressure control components and the transfer function P_u/Q_{load}.

Using parameter variations with the root locus method, it is possible to have the influences of some parameters on the stability of such components. The flow gain is of great importance on the stability as well as the spring stiffness and jet forces. Reducing the flow gain also reduces the flow forces and thus can have adverse effects but generally the flow gain reduction stabilizes the system.

Since a pressure component has always an inner PD controller, the D effect can be well placed in order to stabilize the system. Generally a bigger spool is more stable since the D gain is the active spool section.

The analysis done concerns the control of the pressure in a volume directly connected to the pressure valve. This is not always the case and the controlled volume can be linked to the pressure valve via a hydraulic line. The effects of this line can be of great importance on the stability of the complete system as analysed by Favennec (2002). The analysis presented here has limitations since there is a great influence of the non-linearities. Moreover, the design of pressure valves includes some additional restrictions within the valve body that modify the stability of the system. Also for electrical piloted systems, the effects of the electrical parts are important. However this analysis gives accurate stability tendencies.

Nomenclature and values

D_s	Spool diameter	0.01 m
D_{orif}	Fixed orifice diameter	0.001 m
K_s,K_{spring}	Spring stiffness	1000 N/m
V_{hback}	Counter reaction volume	0.2 cm^3
V_{hutil}	Controlled volume	50 cm^3
M	Spool mass	0.01 kg
C_{qmax}	Fully turbulent discharge coefficient	0.7
λ	Critical flow number	30
α	Jet angle	69°
B	Bulk modulus of the liquid	17000 bar
ρ	Fluid density	850 kg/m^3
ν	Fluid viscosity	50 cSt
A_j,A_{jet}	Equivalent jet force area	[m²]
A_s, A_{spool}	Spool active area	[m²]
A_o, A_{orif}	Fixed orifice cross section	[m²]
C_q	Discharge coefficient	-
$D(s)$	Transfer function denominator	-
F_{jet}	Jet forces	[N]
F_{cmd}	Input force	[N]
G_x	Flow gain	[m^3/s/m]
$G_{\Delta P}$	Flow gain	[m^3/s/Pa]
K_j,K_{jet}	Equivalent jet force stiffness	[N/m]
K_{hb},K_{hback}	Hydraulic stiffness of the	[Pa/m^3]

	counter reaction volume	
K_{hu},K_{hutil}	Hydraulic stiffness of the controlled volume	[Pa/m^3]
P_b,P_{back}	Counter reaction pressure	[Pa]
P_s	Supply pressure	[Pa]
P_u,P_{util}	Controlled volume pressure	[Pa]
Q_o,Q_{orif}	Counter reaction orifice flow rate	[m^3/s]
Q_s,Q_{servo}	Flow rate crossing the valve	[m^3/s]
Q_{load}	Flow rate of load circuit	[m^3/s]
R_{port}	Viscous friction	[Pa/m^3/s]
R_o,R_{orif}	Dissipation linked to the counter reaction restriction	[Pa/m^3/s]
x_s	Spool displacement	[m]
s	Laplace operator	-
λ	Flow number	-

References

Alirand M., Botelle E. and **Sau J.** 2001. Modeling a force control actuator for semi active car damper: pressure controlled valve analysis. *7th Scandinavian Int. Conf. on Fluid Power*, Linköping, Sweden, pp. 313-415.

Baudry X. 2000. Couplage entre approches globale et locale CDF pour la conception d'organes hydrauliques : *Application aux distributeurs hydrauliques et à la compensation des forces de jet. PhD thesis*, Institut National des Sciences Appliquées, Toulouse, France.

Botelle E., Alirand M. and **Sau J.** 2000. Modeling a force control actuator for semi active car damper: flow controlled valve analysis. *4th Advanced Vehicle Control Congress*, Detroit, MI, USA, pp. 313-415.

Favennec G. 2001. Contribution à l'amélioration du cycle de conception du circuit hydraulique de commande d'une boîte de vitesses automatique par simulation et modélisation. *PhD thesis*, Université Claude Bernard, Lyon I, France.

Favennec G., Alirand M. and **Lebrun M.** 2002. Optimal response of pressure reducer and influence of the downstream line dynamics. Submitted for publication to the *2nd FPNI-PhD Symposium*, Modena, Italy.

Green W. L. 1970. The poppet valve – low force compensation. *The 1970 Fluid Power International Conference*, Paper 2, pp. S1-S6.

Handroos H. M. and **Vilenius M. J.** 1990. The utilization of experimental data in modelling hydraulic single stage pressure control valve. *Trans. ASME, Journal of Dynamic Systems, Measurements and Control*, Vol. 112, September 1990, pp. 482-488.

Lebrun M. 1987. A model for a four-way spool valve applied to a pressure control system. *The Journal of Fluid Control*, Vol. 17, No. 4, pp. 38-54.

Louca L. S., Stein J. L., Hulbert G. M. and **Sprague J.** 1997. Proper model generation: an energy-based methodology. *Proceedings of the 3rd Int. Conference on Bond graph Modeling and Simulation, Phoenix*, AZ, January 1997, pp. 1-6.

Mac Cloy D. and **Martin H. R.** 1980. Control of Fluid Power: *Analysis and Design*. Ellis Horwood Ltd Publisher, 2nd Edit.

Maiti R., Surawattanawan P. and **Watton J.** 1999. Performance prediction of a proportional solenoid control pressure relief valve. *4th Japanese Hydraulic and Pneumatic Society Int. Symposium*, Tokyo, Japan, November 1999, pp. 321-326.

Manring N. D. and **Johnson R. E.** 1997. Optimal orifice geometry for a hydraulic pressure-reducing valve. *Trans. ASME, Journal of Dynamic Systems, Measurements and Control*, Vol. 119, September 1997, pp. 467-473.

Mare J. C. 1993. Contribution à la modélisation, la simulation, l'identification et la commande d'actionneurs électrohydrauliques. *PhD thesis*, Université Claude Bernard, Lyon I, France.

Margolis D. L. and **Hennings C.** 1997. Stability of hydraulic motion control systems. *Trans. ASME, Journal of Dynamic Systems, Measurements and Control*, Vol. 119, December 1997, pp. 605-613.

Matsubara M., Takada S., Ikeda M. and **Suzuki K.** 2001. Bond graph based analysis of poppet valve instability. *Proceedings of the 2001 Western Multi Conference*, ICBGM, Phoenix, AR, USA, pp. 1-6.

Merritt H. E. 1967. *Hydraulic Control System*. John Wiley & Sons Publisher.

Rosenberg R. C. and **Zhou T.**, 1988. Power based model insight. *Proceedings of the Winter Annual Meeting of the ASME*, Chicago, IL, vol. DSC-Vol. 8, December 1988, pp. 61-67.

Suzuki K., Nakamura I. and **Thoma J. U.** 1999. Pressure regulator valve by bond graph based analysis of poppet valve instability. *Simulation Practice and Theory*, Vol. 7, pp. 603-611.

Marc Alirand
Born on May 22th 1963 in Saint Etienne (France). PhD on active suspension in 1991 in Mechanical Engineering and Automatic Control at the University Claude Bernard, Lyon. Enter in Imagine in 1990. Specialized in hydraulic components for automotive applications and mostly in chassis engineering.

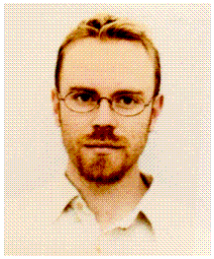

Gwennaël Favennec
Received his PhD in March 2001 on the design and control of the hydraulic control units for a RENAULT automatic gearbox. He is working in the automatic gearbox control department at Renault on electrical and hydraulic actuators for robotized gearbox.

Michel Lebrun
Professor at the University of Lyon I. Received his PhD in 1986 on bond graph technique applied to electro-hydraulic components. Founder and scientific director of the Imagine company.